Review of Scientific Instruments

RESEARCH ARTICLE | AUGUST 31 2018

Developing a long-duration Zn K-α source for x-ray scattering experiments FREE

Special Collection: Proceedings of the 22nd Topical Conference on High-Temperature Plasma Diagnostics

M. J. MacDonald ; A. M. Saunders ; R. W. Falcone; W. Theobald; O. L. Landen ; T. Döppner

Rev. Sci. Instrum. 89, 10F109 (2018)
https://doi.org/10.1063/1.5039365
CHORUS

AIP Publishing

Developing a long-duration Zn K-α source for x-ray scattering experiments

M. J. MacDonald,[1,a)] A. M. Saunders,[1] R. W. Falcone,[1] W. Theobald,[2] O. L. Landen,[3] and T. Döppner[3]
[1]*Department of Physics, University of California, Berkeley, California 94720, USA*
[2]*Laboratory for Laser Energetics, University of Rochester, Rochester, New York 14623, USA*
[3]*Lawrence Livermore National Laboratory, Livermore, California 94550, USA*

(Presented 16 April 2018; received 7 May 2018; accepted 25 June 2018; published online 31 August 2018)

We are developing a long-duration K-α x-ray source at the Omega laser facility. Such sources are important for x-ray scattering measurements at small scattering angles where high spectral resolution is required. To date, He-α x-ray sources are the most common probes in scattering experiments, using ns-class lasers to heat foils to keV temperatures, resulting in K-shell emission from He-like charge states. The He-α spectrum can be broadened by emission from multiple charge states and lines (e.g., He-like, Li-like, Be-like). Here, we combine the long duration of He-α sources with the narrow spectral bandwidth of cold K-α emission. A Ge foil is irradiated by the Omega laser, producing principally Ge He-α emission, which pumps Zn K-α emission at 8.6 keV from a nearby Zn layer. Using this technique, we demonstrate a long-duration Zn K-α source suitable for scattering measurements. Our experimental results show a 60% reduction in spectral bandwidth compared to a standard Zn He-α source, significantly improving the measurement precision of scattering experiments with small inelastic shifts. *Published by AIP Publishing.* https://doi.org/10.1063/1.5039365

I. INTRODUCTION

X-ray Thomson scattering (XRTS) is a common diagnostic technique used to measure the conditions of dense plasmas.[1] XRTS spectra consist of elastic and inelastic components, where the strength of the elastic component contains information on the number of bound electrons and the ion-ion structure factor, and the shape of the inelastic spectrum is related to plasma density and temperature. At low scattering angles, where the momentum transfer to scattered photons is small, XRTS can probe collective electron oscillations (plasmons) in dense plasmas.[2] In this regime, precise XRTS measurements are more challenging because the inelastic energy shift is relatively small, often overlapping with elastic scattering. Without precise knowledge of the probe spectrum, deconvolving and interpreting the inelastic peak result in larger uncertainties. By reducing the spectral bandwidth of the probe source, the inelastic spectrum can be known more precisely, significantly improving XRTS measurement precision at small scattering angles.

Most XRTS experiments to date at large laser facilities, such as the Omega at the Laboratory for Laser Energetics or the National Ignition Facility (NIF) at Lawrence Livermore National Laboratory, have used He-α x-ray sources,[2–5] with Zn He-α being a common choice because of its ability to penetrate high-density plasmas. To produce He-α x-rays, a laser incident upon a metal foil creates a plasma at keV temperatures. The spectral bandwidth of He-α x-ray sources is typically greater than 100 eV, limiting the precision of x-ray scattering measurements. To illustrate this point, Fig. 1(a) shows x-ray emission simulations using FLYCHK[6] for Zn plasmas at temperatures of 3–5 keV and electron densities of 1×10^{21} cm^{-3}, 10% the critical electron density for 351 nm laser radiation. Figure 1(b) shows the same spectra assuming 45 eV full width at half maximum (FWHM) spectrometer resolution.

By contrast, K-α emission from neutral or near-neutral atoms consists of two spectral lines with well-known energies (K-$\alpha_{1,2}$). For mid-Z elements, these lines are separated by 5–25 eV and are insensitive to heating until M-shell ionization begins (T $\approx$ 100 eV for Zn). XRTS measurements using a K-α probe have been demonstrated using a short-pulse laser system.[7] However, short-pulse lasers generate high backgrounds due to the presence of high-energy particles created by the ultra-intense laser-matter interaction[8] and the probe timing is limited by the duration of the laser pulse (1–10 ps). In this paper, we present a proof-of-principle experiment demonstrating a long-duration ($\approx$1 ns) Zn K-α source pumped by a Ge He-α x-ray source. This method enables the use of nanosecond laser systems to produce an x-ray source with a narrow spectral bandwidth and reduced background compared to x-ray sources driven by short-pulse lasers.

II. CONVERSION EFFICIENCY OPTIMIZATION

Due to the small Thomson scattering cross section ($\sigma_{Th} = 6.65 \times 10^{-25}$ cm^2), bright probe sources are required for XRTS measurements to obtain a sufficient signal-to-noise ratio. In order to minimize the loss of total probe energy in the conversion from He-α to K-α x-rays, the target needs to be designed to maximize the K-α yield.

The conceptual design of the long-duration K-α x-ray source consists of two layers: a He-α x-ray source (pump)

Note: Paper published as part of the Proceedings of the 22nd Topical Conference on High-Temperature Plasma Diagnostics, San Diego, California, April 2018.

a)macdonm@berkeley.edu

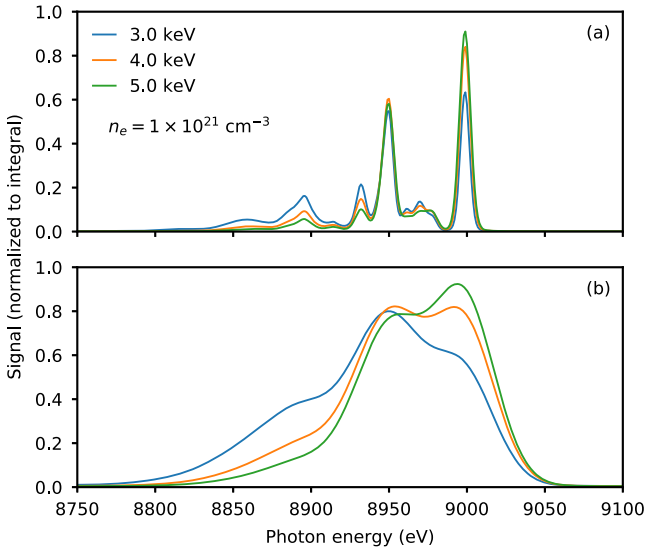

FIG. 1. (a) Simulated x-ray emission for Zn at temperatures of 3–5 keV and $n_e = 1 \times 10^{21}$ cm^{-3} using FLYCHK, showing the emission lines resulting from He-like, Li-like, and Be-like Zn ions. (b) The same spectra assuming 45 eV FWHM spectral resolution.

layer and a converter layer that absorbs the pump radiation and produces K-α x-rays. An optional middle buffer layer can be added to reduce heating of the converter layer. The thicknesses of each layer can be optimized to maximize the K-α yield. The He-α emission layer needs to be as thin as possible to minimize absorption of the pump radiation while preventing burn-through during the laser drive. If a buffer layer is included, it should be a low-Z material to minimize absorption of the pump radiation and as thin as possible to minimize the distance between the pump and converter layers to maximize the fraction of pump x-rays captured by the converter layer.

The optimal thickness of the K-α converter layer is determined by balancing the increased pump absorption from increasing the layer thickness with the absorption of K-α x-rays through the remaining layer thickness. Here, we consider a 1D model of the converter layer to calculate the optimal converter layer thickness to maximize conversion efficiency. A more detailed analysis would be required to accurately account for pump x-rays entering the converter layer at different angles, but a simple 1D analysis is sufficient to estimate the optimal converter layer thickness. The ratio of emitted K-α fluorescence x-rays (γ_f) to incident He-α x-rays (γ_p) by a given volume element of length dx is given by[9]

$$\left(\frac{\gamma_f}{\gamma_p}\right)_{dx} = e^{-\mu_p \rho x}\left(1 - e^{-\mu_{p,pe}\rho dx}\right) f_{K\alpha} e^{-\mu_f \rho (L-x)}, \quad (1)$$

where x is the position in the layer, ρ is the material density, μ is the mass attenuation coefficient, $f_{K\alpha}$ is the fraction of excited atoms decaying via K-α emission, and L is the thickness of the converter layer. The subscripts p and f refer to the pump and fluorescence x-rays, respectively, and p, pe refers to only the K-shell component of the photoelectric absorption coefficient. The four terms in Eq. (1) account for the absorption of the pump x-rays before reaching the volume element, the fraction of x-rays absorbed by the element, the fraction of excited atoms emitting K-α photons, and the absorption of the fluorescence x-rays leaving the layer, respectively.

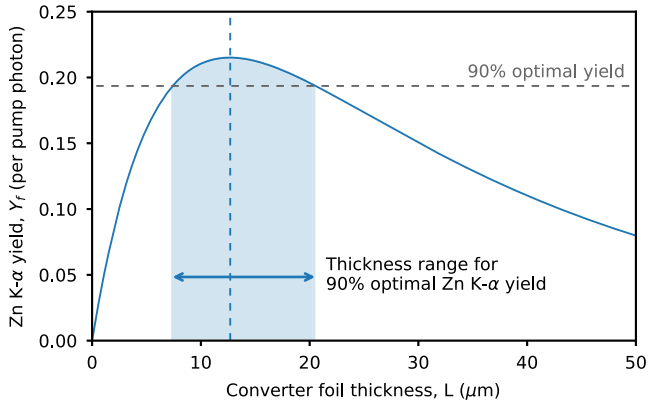

FIG. 2. Zn K-α yield calculations for a Ge He-α pump, showing the optimal Zn thickness and the range of thicknesses for 90% optimal conversion efficiency.

The total K-α yield (relative to the incident pump flux) is calculated by integrating over the length of the converter layer, given by

$$Y_f(L) = f_{K\alpha}\left(\frac{\mu_{p,pe}}{\mu_p - \mu_f}\right)\left(e^{-L\rho\mu_f} - e^{-L\rho\mu_p}\right). \quad (2)$$

Equation (2) is shown in Fig. 2 for the case of a Ge He-α pump and a Zn converter layer. Solving for the maximum yield from Eq. (2) gives the optimal converter layer thickness in terms of the mass attenuation coefficients and the density of the converter layer,

$$L_{opt} = \frac{\log(\mu_p/\mu_f)}{(\mu_p - \mu_f)\rho}. \quad (3)$$

The parameters used in these calculations are summarized in Table I. We find that the optimal converter layer thickness for a Zn converter layer pumped by Ge He-α x-rays is 12.7 μm. The optimal layer thickness is a shallow maximum, with the range of 7.4–20.5 μm, resulting in 90% optimal Zn K-α yield or greater.

This same analysis applies to other pump-fluorescer pairs to produce K-α sources at different photon energies, where the values in Table I would need to be recalculated. In general, the pump emission energy should be close to the K-edge of the fluorescer element for efficient absorption but needs to be above the K-edge in order to produce K-shell vacancies. In cases where preheating of the converter foil may be an issue,

TABLE I. Parameters used in Sec. II.

Parameter	Value
Zn K-α_1, K-α_2 energies (eV)	8639, 8616
Ge He-α central energy (eV)	10250
Zn density (ρ) (g/cm^3)	7.16
K-α emission fraction[10] ($f_{K\alpha}$)	0.3786
Total attenuation, Ge He-α[11] (μ_p) (cm^2/g)	217.9
K-shell photoelectric absorption, Ge He-α[11] ($\mu_{p,pe}$) (cm^2/g)	187.7
Total attenuation, Zn K-α[11] (μ_f) (cm^2/g)	46.02

the increased K-edge energy should be accounted for when choosing the pump source.

III. EXPERIMENTAL SETUP

A first proof-of-principle experiment was conducted at the Omega laser facility. The design of the layered target used in this experiment is shown in Fig. 3. Ge He-α x-rays were produced by a 6 μm Ge foil, and the converter layer was a 10-μm-thick Zn foil. The Ge backlighter stack (consisting of 6 μm Ge, 200 μm graphite, and 6 μm Ge) was chosen because it is a standard backlighter for other campaigns and was available for this experiment. The graphite layer and additional Ge layer prevented preheat of the Zn while not significantly attenuating the Ge He-α pump emission. A 50-μm-thick Ta collimator was added to the target with a 100 μm slit (1600 μm in length) to limit the source size of the emitting Zn K-α x-rays in the dispersion direction.

Eight beams of the Omega laser irradiated the Ge foil to produce Ge He-α emission centered at 10.25 keV. A total of 3.8 kJ of laser energy in the third harmonic (3ω = 351 nm) was delivered to the target in a 1-ns square pulse. The eight beams had three different phase plates, four E-IDI-300, three E-SG10-100, and one E-SG10-300, overlapped on the Ge foil to produce a roughly circular super-Gaussian spot with a FWHM of 300 μm and intensity of approximately 2×10^{16} W/cm^2. At this intensity, the conversion efficiency from laser energy to Ge He-α x-rays is approximately 0.002.[12]

IV. SPECTRAL RESULTS

The zinc spectrometer (ZSPEC) at Omega[4] configured with a flat highly ordered pyrolytic graphite (HOPG) crystal was fielded to measure the Ge He-α and Zn K-shell emission in this experiment. The ZSPEC uses a microchannel plate (MCP) coupled to a charge-coupled device (CCD) to provide time-gated measurements. The ZSPEC was operated with a 180 ps integration time to measure the peak emission of the foil while preventing contamination from the Ge plasma expanding around the foil at late times. The blast shield (placed between the target and the crystal) consisted of 750 μm of Be and 75 μm of polypropylene, and the rear filter (between the crystal and the detector) was 300 μm of Al and 500 μm of Be. The alignment of the ZSPEC was adjusted to measure 8000–11 000 eV, centering the Zn K-shell emission and the Ge He-α emission on the crystal to avoid reduced reflectivity near the edges of the crystal.

The spectral dispersion of the ZSPEC was calculated using ray tracing to account for the spatial offset of the Ge plasma and the Zn converter layer. A sample spectrum taken at 450 ps (360–540 ps integration time) after the start of the laser pulse is shown in black in Fig. 4. Spectra were collected in the range of 110–790 ps with similar results, confirming that the Zn K-shell emission remained on throughout the duration of the pump emission as expected. The combined fit to the data (dashed red line) includes three components illustrated by shaded regions: the Ge He-α pump emission (orange), the Zn K-shell emission (blue), and the background continuum emission (light gray).

The relative energy in Zn K-shell emission compared to the Ge He-α emission was determined by fitting the calibrated ZSPEC data, including the filter transmissions for each line. The filter transmission for the Zn K-shell lines only includes the detector filters, whereas the Ge He-α and thermal background emission are also attenuated by the buffer layers of the target (graphite and Ge) and the Zn converter layer. The line shapes of each line were assumed to be Gaussian, with the 45 eV spectral resolution of the ZSPEC applied to each line.

A. Spectral bandwidth

The primary goal of this experiment was to reduce the spectral bandwidth of the probe radiation for XRTS experiments. To make a fair comparison between these results and a typical XRTS probe spectrum used at Omega, we compare the measured Zn K-α spectrum to a Zn He-α probe spectrum measured on the same spectrometer, shown in Fig. 5.

Our data demonstrate a 60% reduction in the FWHM of the K-α emission compared to the Zn He-α spectrum, 51 eV compared to 128 eV. We do not see the individual K-α

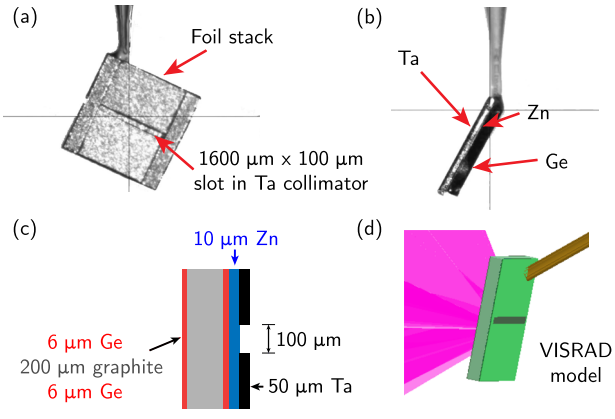

FIG. 3. [(a) and (b)] Pictures of the experimental target, showing the foil stack and the 100 μm Ta slit aperture to reduce the source size of the Ge He-α and Zn K-α x-rays. (c) Thicknesses of each layer in the foil stack. (d) VISRAD model of the target including the eight Omega beams heating the Ge foil.

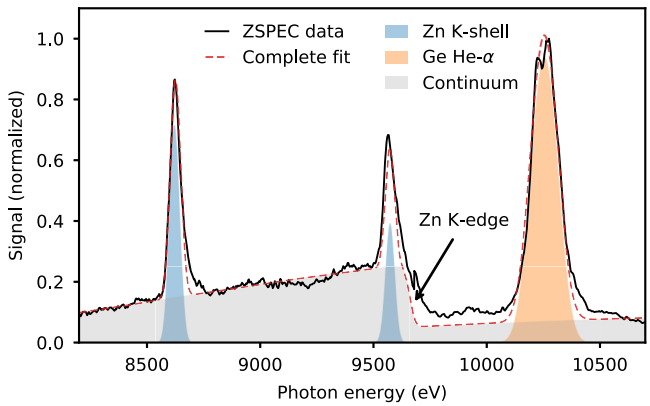

FIG. 4. Full calibrated and background-subtracted ZSPEC spectrum showing the pump Ge He-α peak and the two resulting fluorescence lines from Zn (K-α and K-β).

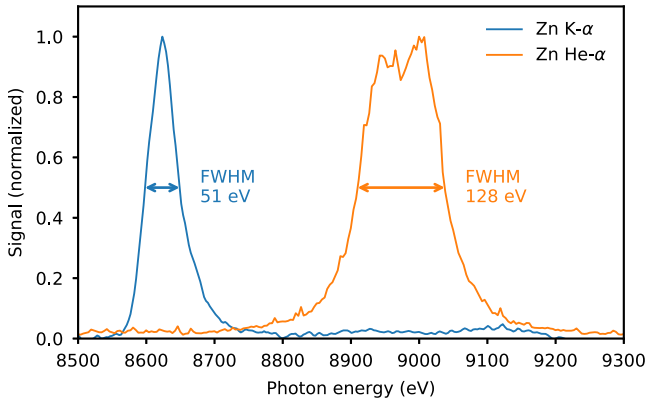

FIG. 5. The Zn K-α measured in the experiment described above and a Zn He-α spectrum from a directly irradiated Zn foil at Omega on the same spectrometer, showing a reduction in FWHM from 128 eV to 51 eV. The spectra are normalized to highlight the improvement in the spectral bandwidth.

emission lines due to the 45 eV spectral resolution of the ZSPEC (K-$\alpha_{1,2}$ at 8639 and 8616 eV, respectively). By contrast, the He-α spectrum consists of many spectral lines from a distribution of highly charged Zn ions (e.g., He-like, Li-like, Be-like), as illustrated by the FLYCHK simulations in Fig. 1, resulting in a much broader spectrum. The extended tail on the high energy side of each spectrum is a result of depth broadening in the 2-mm-thick HOPG crystal.[13]

B. Conversion efficiency

To estimate the fraction of total emitted Ge He-α photons resulting in Zn K-α emission (γ_f/γ_p), we need to calculate the solid angle subtended by the converter layer as seen by the pump emission (Ω_f), the transmission of the pump photons to the converter layer (t_p), and the yield fraction (Y_f) in the converter layer from Eq. (2). The fraction of emitted fluorescence photons is given by

$$\left(\frac{\gamma_f}{\gamma_p}\right)_{total} = \left(\frac{\Omega_f}{4\pi}\right) t_p Y_f. \quad (4)$$

Here, we have a 100 μm × 1600 μm active area of the converter layer (defined by the Ta slit aperture) placed 210 μm from the Ge He-α emission, resulting in $\Omega_f/4\pi = 0.07$. To account for the range of angles the pump x-rays travel through the buffer layer (Ge and graphite), we calculate the average transmission from a point source centered at the Ge emission spot to each point on the Zn foil, yielding an average transmission of $t_p = 0.4$. For the fractional yield of K-α photons, we use Eq. (2) for a 10 μm Zn converter foil, $Y_f = 0.21$. Using these values, we estimate a conversion efficiency from Ge He-α to Zn K-α of $\gamma_f/\gamma_p = 0.006$. This yield could be increased by reducing the distance between the pump and converter layers, increasing both Ω_f and t_p.

Accounting for the difference in total filter transmission of the two lines (0.035 for Zn K-α and 0.020 for Ge He-α) and the fraction of Ge He-α emission visible through the Ta slit aperture, the best fit to the data corresponds to $\gamma_f/\gamma_p = 0.07$, a factor of 10 larger than the predicted value. From the measured spectrum, it is clear that a significant amount of continuum emission is absorbed by the Zn layer (absorption above the Zn K-edge at 9659 eV). Accounting for pumping from the continuum up to 11 keV (limited by the detector), we get $\gamma_f/\gamma_p = 0.02$. The remaining factor of three discrepancy between the measured and theoretical values can be attributed to the additional high-energy background (fast electrons, x-ray emission above 11 keV) and additional pumping not included in our 1D model.

V. XRTS ANALYSIS

To demonstrate the impact of the improvement the reduced spectral bandwidth of the Zn K-α source makes on XRTS spectra, we consider the geometry of an experiment recently conducted by the authors at the Omega laser. In this experiment, a carbon foam sample is heated by a planar shock wave to a shocked density of 800 mg/cm^3 and probed using XRTS at a scattering angle of 90°. Figure 6 shows simulated XRTS spectra of carbon foam heated to temperatures of 20–40 eV in this geometry for the cases of (a) the Zn K-α probe measured in this experiment and (b) a Zn He-α probe spectrum.

In the case of the He-α probe, the inelastic peak overlaps with the probe spectrum because the Compton shift is not large enough to separate the inelastic and elastic components. Any uncertainties in the probe spectrum for the measurement would lead to systematic uncertainties in the inelastic component. Analysis of the K-α probe spectrum could be completed with greater certainty because the probe spectrum is clearly separated from the Compton-shifted inelastic peak.

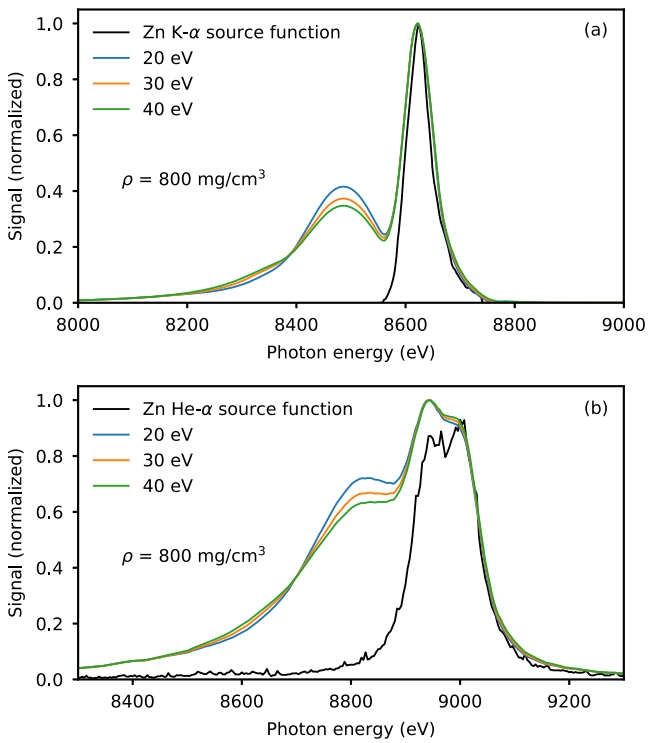

FIG. 6. Simulated XRTS spectra at a scattering angle of 90° for a recent Omega experiment probed by (a) the measured K-α source and (b) a standard Zn He-α source. The reduced bandwidth in (a) significantly improves the separation of the elastic and inelastic scattering components.

VI. CONCLUSION

We presented a design to produce a long-duration K-α x-ray source for x-ray scattering experiments at large-scale long-pulse laser facilities. The design considerations for the x-ray pumped converter foil were explored, and the optimal converter foil thickness was calculated for the case of Zn K-α pumped by a Ge He-α source. We presented experimental results from the Omega laser facility, demonstrating a reduction in spectral bandwidth of 60% compared to a conventional Zn He-α source.

The design of the proof-of-principle experiment presented in this paper can be improved in several ways to increase K-α yield. First, the thickness of the buffer layer in this design can be significantly reduced (or even removed) to increase the coupling between the pump and converter layers. If the layer is removed, the fractional solid angle in Eq. (4) can approach 0.5 (compared to 0.07 in this setup). Second, the conversion efficiency from laser energy to Ge He-α can be improved by using a pre-pulse and reducing the laser intensity. By reducing the intensity to 1×10^{15} W/cm^2, conversion efficiencies up to 0.015 have been demonstrated for Ge He-α (compared to 0.002 here)[14] while also reducing the thermal background. Including these optimizations, the conversion efficiency from laser energy to Zn K-α could approach 10^{-3}. Finally, the thermal background could be almost entirely eliminated by removing the direct line-of-sight between the pump source and the scattering sample by using a more sophisticated probe target design, reducing the background in the resulting x-ray scattering spectra.

These results demonstrate the ability to create long-duration K-α x-ray sources at large-scale laser facilities that can be used to improve the measurement precision in x-ray scattering experiments. This new probe source is particularly useful for experimental platforms with constrained x-ray scattering geometries where the inelastic shift is small.

ACKNOWLEDGMENTS

The authors would like to thank the Omega operations staff for a successful experimental campaign and D. B. Thorn for insightful discussions regarding spectrometer calibration and data interpretation. This material is based upon the work supported by the U.S. Department of Energy, Office of Science, Office of Basic Energy Sciences under Award No. DE-SC0018298, under the auspices of the U.S. Department of Energy by Lawrence Livermore National Laboratory under Contract No. DE-AC52-07NA27344, performed under the Stewardship Science Graduate Fellowship program support Contract No. DE-NA0002135, and supported by Laboratory Directed Research and Development (LDRD) Grant No. 18-ERD-033. Laser system time provided by the LBS program at the LLE Omega Facility.

[1] S. H. Glenzer and R. Redmer, Rev. Mod. Phys. **81**, 1625 (2009).
[2] T. Döppner, O. Landen, H. Lee, P. Neumayer, S. Regan, and S. Glenzer, High Energy Density Phys. **5**, 182 (2009).
[3] H. J. Lee, P. Neumayer, J. Castor, T. Döppner, R. W. Falcone, C. Fortmann, B. A. Hammel, A. L. Kritcher, O. L. Landen, R. W. Lee, D. D. Meyerhofer, D. H. Munro, R. Redmer, S. P. Regan, S. Weber, and S. H. Glenzer, Phys. Rev. Lett. **102**, 115001 (2009).
[4] A. L. Kritcher, T. Döppner, C. Fortmann, T. Ma, O. L. Landen, R. Wallace, and S. H. Glenzer, Phys. Rev. Lett. **107**, 015002 (2011).
[5] D. Kraus, D. A. Chapman, A. L. Kritcher, R. A. Baggott, B. Bachmann, G. W. Collins, S. H. Glenzer, J. A. Hawreliak, D. H. Kalantar, O. L. Landen, T. Ma, S. Le Pape, J. Nilsen, D. C. Swift, P. Neumayer, R. W. Falcone, D. O. Gericke, and T. Döppner, Phys. Rev. E **94**, 011202 (2016).
[6] H.-K. Chung, M. Chen, W. Morgan, Y. Ralchenko, and R. Lee, High Energy Density Phys. **1**, 3 (2005).
[7] A. L. Kritcher, P. Neumayer, J. Castor, T. Döppner, R. W. Falcone, O. L. Landen, H. J. Lee, R. W. Lee, E. C. Morse, A. Ng, S. Pollaine, D. Price, and S. H. Glenzer, Science **322**, 69 (2008).
[8] P. M. Nilson, J. R. Davies, W. Theobald, P. A. Jaanimagi, C. Mileham, R. K. Jungquist, C. Stoeckl, I. A. Begishev, A. A. Solodov, J. F. Myatt, J. D. Zuegel, T. C. Sangster, R. Betti, and D. D. Meyerhofer, Phys. Rev. Lett. **108**, 085002 (2012).
[9] M. J. MacDonald, P. A. Keiter, D. S. Montgomery, H. A. Scott, M. M. Biener, J. R. Fein, K. B. Fournier, E. J. Gamboa, G. E. Kemp, S. R. Klein, C. C. Kuranz, H. J. LeFevre, M. J.-E. Manuel, W. C. Wan, and R. P. Drake, J. Appl. Phys. **120**, 125901 (2016).
[10] N. Broll, X-Ray Spectrom. **15**, 271 (1986).
[11] M. J. Berger, J. H. Hubbell, S. M. Seltzer, J. Chang, J. S. Coursey, R. Sukumar, D. S. Zucker, and K. Olsen, see http://physics.nist.gov/xcom for XCOM: Photon Cross Section Database.
[12] J. Workman and G. A. Kyrala, Proc. SPIE **4504**, 168 (2001).
[13] T. Döppner, P. Neumayer, F. Girard, N. L. Kugland, O. L. Landen, C. Niemann, and S. H. Glenzer, Rev. Sci. Instrum. **79**, 10E311 (2008).
[14] M. Barrios, K. Fournier, S. Regan, O. Landen, M. May, Y. Opachich, K. Widmann, D. Bradley, and G. Collins, High Energy Density Phys. **9**, 626 (2013).